PCCP

Accepted Manuscript

This is an *Accepted Manuscript*, which has been through the Royal Society of Chemistry peer review process and has been accepted for publication.

Accepted Manuscripts are published online shortly after acceptance, before technical editing, formatting and proof reading. Using this free service, authors can make their results available to the community, in citable form, before we publish the edited article. We will replace this *Accepted Manuscript* with the edited and formatted *Advance Article* as soon as it is available.

You can find more information about *Accepted Manuscripts* in the Information for Authors.

Please note that technical editing may introduce minor changes to the text and/or graphics, which may alter content. The journal's standard Terms & Conditions and the Ethical guidelines still apply. In no event shall the Royal Society of Chemistry be held responsible for any errors or omissions in this *Accepted Manuscript* or any consequences arising from the use of any information it contains.

ROYAL SOCIETY OF CHEMISTRY

www.rsc.org/pccp

Specific ion effects on the electrokinetic properties of iron oxide nanoparticles: experiments and simulations

Fernando Vereda,[a]* Alberto Martín-Molina,[a] Roque Hidalgo-Alvarez,[a] and Manuel Quesada-Pérez[b]

a) Grupo de Física de Fluidos y Biocoloides, Departamento de Física Aplicada, Facultad de Ciencias, Universidad de Granada, 18071 Granada, Spain.

b) Departamento de Física, Escuela Politécnica Superior de Linares, Universidad de Jaén, 23700, Linares, Jaén, Spain.

*fvereda@ugr.es

Tel. 34-958240025

Fax: 34-958243214

Keywords: Ion specificity, magnetite, Hofmeister series, iron oxide, Monte Carlo simulations

Physical Chemistry Chemical Physics Accepted Manuscript

ABSTRACT.

We report experimental and simulation studies on specific ion phenomena in aqueous colloidal suspensions of positively charged, bare magnetite nanoparticles. Magnetite has the largest saturation magnetization among iron oxides and a relatively low toxicity, which explains why it has been used in multiple biomedical applications. Bare magnetite is hydrophilic and the sign of the surface charge can be changed by adjusting pH, its isoelectric point being in the vicinity of pH = 7. Electrophoretic mobility of our nanoparticles in the presence of increasing concentrations of different anions showed that anions regarded as *kosmotropic* are more efficient at decreasing, and even reversing, the mobility of the particles. If the anions were ordered according to the extent to which they reduced particle mobility, a classical Hofmeister series was obtained with the exception of thiocyanate, whose position was altered. Monte Carlo simulations were used to predict the diffuse potential of magnetite in the presence of the same anions. The simulations took into account ion volume, and electrostatic and dispersion forces among the ions and between the ions and the solid surface. Even though no fitting parameters were introduced and all input data was estimated from Lifshitz theory for van der Waals forces or obtained from the literature, the predicted diffusion potentials of the different anions followed the same order as the mobility curves. Results suggest that ionic polarizabilities and sizes are responsible to a great extent for the specific ion effects on the electrokinetic potential of oxide iron particles.

Physical Chemistry Chemical Physics Accepted Manuscript

INTRODUCTION.

Specific ion effects have been extensively studied since 1888, when Hofmeister discovered ion specific effects on the precipitation of purified egg white.[1–6] Hofmeister showed that salts with the same cation but different anions precipitated the protein at different concentrations. This behaviour was also observed with some other colloidal suspensions.[1–6] Accordingly, the effectiveness of different anions with the cation fixed, or of cations with a fixed anion, can be ordered reproducibly in the so-called Hofmeister series. In colloid science and biochemistry, there is a plethora of experiments showing that ions with the same valence can induce very different behaviours. Such experiments include protein solubility, critical micelle concentration, surface tension, forces between charged surfaces and electrophoretic mobilities, to which we will pay special attention in this work.[1–6] Regardless of the huge number of studies over the years, Hofmeister phenomena are still gaining popularity nowadays. This is due to, amongst other things, aqueous ion-containing interfaces are ubiquitous and play a key role in a plethora of physical, chemical, atmospheric, and biological processes.[7] Hofmeister phenomena in bulk phases, in surfactant-based systems and at interfaces, in gels, in proteins and enzymes, and in real biological systems and medicine are some of the examples which have been extensively analysed in the last decades.[1–6] Among these examples, ion specificity effects focused on biology are those that have mostly attracted the attention of the *Hofmeister community* nowadays.[1,2,8] This is why there is a renewed interest in Hofmeister phenomena in colloids with biological applications.

Precisely, our goal was to study specific ion effects of iron oxide nanoparticles. Iron oxides (a general term that often includes iron oxyhydroxides) present many polymorphs with a variety of electronic and magnetic properties, and are relatively easy, and inexpensive, to synthesize in the laboratory. They are currently the subject of intense research for multiple applications,[9] including water splitting for the production of H_2, anodes for Li-ion batteries, catalysis, and above all, for many applications in biomedical or biotechnological areas. Iron oxide phases with a relatively strong magnetic response (mainly the magnetite (Fe_3O_4)/maghemite (γ-Fe_2O_3) system) have been studied[10,11] for drug and gene delivery, for protein and DNA separation, for tissue engineering, as contrast factors for MRI imaging, or for magnetic hyperthermia. Magnetic iron oxide nanoparticles are especially attractive for biomedical uses because

Physical Chemistry Chemical Physics Accepted Manuscript

they can be manipulated with external magnetic fields and because of their relatively low toxicity.

Despite the technological relevance of iron oxide nanoparticles in applications that involve the use of aqueous suspensions, we have not been able to find many studies or accounts on ion specificity in these systems. Most of those studies are dedicated to hematite,[12–14] a weakly ferromagnetic iron oxide at room temperature. Regarding magnetite, we came across a study by Dixon[15] on the interaction of alkaline-earth cations with the magnetite water interface. The differences observed between the different divalent cations were explained in terms of ion radii and their degree of hydration.

From a theoretical point of view, the ionic distribution around a charged colloid immersed in an electrolytic solution is named electric double layer (EDL). Classical models of EDL are based on the Poisson-Boltzmann (PB) equation, which do not account for ionic specificity. As a consequence, the standard Derjaguin–Landau–Verwey–Overbeek (DLVO) theory of colloids is unable to explain ion specific forces between colloidal particles.[16] Similarly, those electrokinetic models based on the PB equation cannot explain, a priori, why ions with identical valence cause different behaviours. In order to overcome these deficiencies, effective or fitting parameters are usually included in the classical theories of electrolytes in order to capture the specificity of ions.[17] With this approach, however, the capability of prediction of this kind of phenomenological approaches vanishes. In contrast, Ninham and coworkers pioneered the inclusion of the dispersion forces with associated hydration effects acting on ions in the colloidal formalisms (see review articles [1,2,4,5] and references cited therein). The resulting theories show how specific ion effects are much more sensitive to anions than to cations, indicating also that Hofmeister effects depend on an interplay between specific surface chemistry, surface charge density, pH, buffer, and counterion with polarizabilities and ion size.[5] Accordingly, mean field theories have been recently reformulated by using a modified PB equation that accounts for non-electrostatic interactions due to the size and the polarizability of each ion.[18–20] Although many of these theoretical predictions qualitatively agree with experimental results, a major comprehension of the different models is required to better understand the physicochemical aspects derived from ionic specificity. For instance, sophisticated formalisms do not allow for a systematic analysis of the interplay between the different contributions that influence the Hofmeister series.[21] Under this scenario, computer

Physical Chemistry Chemical Physics Accepted Manuscript

simulations appear as a useful tool. On one hand, simulations permit to test the validity of the models under hardly accessible conditions in experiments. On the other hand, systematic studies can be performed via simulations in order to assess the weight of different contributions presented in the theoretical models. Unfortunately the use of simulations to study the specific ion effects on colloids is scarce. For instance, Tavares *et al*. and Böstrom *et al*. adopted the primitive model to study the effect of van der Waals interactions on forces between charged surfaces by computer simulations.[22,23] These authors also used Molecular Dynamic (MD) simulations to parametrise ionic potentials in a generalized Poisson-Boltzmann equation.[24] MD simulations were also used to study the ionic specificity in the interaction of monovalent ions with hydrophobic and hydrophilic colloids.[25]

Inspired by the simulations based on the primitive model and performed by Tavares *et al*. and Böstrom *et al*., we previously evaluated the effect of ionic dispersion forces on the EDL of colloids by means of Monte Carlo (MC) simulations.[26,27] The results shown therein revealed that ionic van der Waals forces can sometimes contribute to the ion specificity of electrokinetic properties of model colloids, although their relevance strongly depends on ion size. Moreover, this subtle balance between polarizability of ions and their hydrated size was used to partially justify ion specific effects observed in the electrophoretic mobility of latex particles by Lopez-Leon *et al.*[17]

To sum up, our goal was to explore ion specific effects on iron oxide nanoparticles through both experiments and theoretical simulations. Experimentally, we synthesized magnetite nanoparticles and measured their electrophoretic mobility in the presence of several anions taken from the representative Hofmeister series given by Lopez-Leon an coworkers:[17]

$citrate^{3-} > SO_4^{2-} > PO_4H^{2-} > F^- > CH_3COO^- > Cl^- > Br^- > I^- > NO_3^- > ClO_4^- > SCN^-$

(kosmotropic anions) (chaotropic anions)

The interactions between the magnetite surface and the anions was also studied by means of MC simulations in order to complement the experimental data and to deepen our understanding of the specific ion effects on the electrokinetic properties of this important colloidal system. Particularly we want to find out if the Lifshitz theory for van der Waals forces succeeds in justifying (and even predicting) the Hofmeister series of magnetite nanoparticles.

Accordingly, the work is organized as follows. In the next section, the experimental systems and procedures are presented. Next, the technical details of the model and

Physical Chemistry Chemical Physics Accepted Manuscript

simulations are outlined. Subsequently, the results are shown and discussed and some conclusions are finally drawn.

EXPERIMENTAL SYSTEMS.

Synthesis of the iron oxide nanoparticles. Magnetite was chosen as the iron oxide phase due to our previous experience with this material, and because reliable information on its interfacial properties and on its dielectric response[28–30] that was needed for the computer simulations was found in literature.

The magnetite nanoparticles were prepared in our laboratory by the oxidative aging of a ferrous hydroxide precipitate with nitrate in aqueous media. This method has been thoroughly described in the past[31,32] for the preparation of magnetite. It is well known that if the process is carried out in an excess of OH^-, i.e. at a relatively large basic pH far from the isoelectric point of magnetite (ca. 6.5 – 7.0), the resulting particles are single crystals with sizes between 50 and 200 nm. We carried out the process at an excess of OH^- of 0.075 M.[33] Doubly distilled water was used for the preparation of the solutions: the first solution, containing KNO_3 (Scharlau, reagent grade, 99%) and KOH (Panreac, chemically pure, 90%), was introduced in a 5-neck jacketed reactor and purged with N_2 for an hour to get rid of dissolved atmospheric O_2. At that point, a $FeSO_4$ $7H_2O$ (Sigma Aldrich, reagent grade, 99%) solution was prepared in H_2SO_4 0.01 M that had also been purged for an hour with N_2. Upon the mixing of the two solutions, which resulted in the immediate formation of the dark green ferrous hydroxide precipitate, the circulation of hot water through the jacket of the reactor was started. This made the temperature of the reactant mixture reach 90 ^oC in approximately 12 minutes. The final concentrations of OH^-, NO^{3-} and Fe^{2+} were 0.125 M, 0.20 M and 0.025 M respectively, and the total volume of the reactant mixture was 800 mL. The system was kept at 90 ^oC for 4 hours. The main differences between this synthesis process and those reported in the past[31,33] relied on the fact that this time moderate mechanical stirring of the reactant mixture and a N_2 flow were maintained during the 4 hours of aging. The N_2 flow implied that the pressure inside the reactor was practically atmospheric pressure, whereas in previous reports the process was carried out in sealed screw-cap flasks and the pressure must have been higher. Its value, however, was not reported.

Physical Chemistry Chemical Physics Accepted Manuscript

After the 4 hours of aging, the final black precipitate was washed several times with distilled water with the help of a permanent magnet to speed the separation of the particles. The particles were finally stored at 5 ^{o}C in ethanol.

Preparation of aqueous suspensions for electrophoretic mobility measurements. Over time the nanoparticles stored in ethanol settled down. When needed, the sediment would be redispersed in the ethanol supernatant by means of stirring and sonication, and small aliquots of this magnetite-ethanol dispersion were dried at room temperature. The resulting black powder would be dispersed in the appropriate aqueous solution for the electrophoresis measurements.

Electrophoretic mobility as a function of pH. The magnetite nanoparticles in the dried powder form were dispersed in 2 mM $NaNO_3$ solutions. The pH of these suspensions was lowered with HNO_3 or raised with NaOH, and the electrophoretic mobility was measured at the resulting pH values.

Electrophoretic mobility in the presence of various electrolytes. Because we wanted to study the specific behaviour of several anions in the iron oxide-water interface, all measurements reported in this manuscript were carried out at pH = 4 so that the nanoparticles surface was positively charged and the anions were counterions. The dry powder was dispersed in a HNO_3 aqueous solution at pH = 4 to obtain a stock suspension of nanoparticles. Meanwhile, solutions of a variety of electrolytes (NaSCN, $NaClO_4$, CH_3COONa, Na_2SO_4, $Na_3C_6H_5O_7$) were prepared with concentrations of 5 mM, 20 mM, 50 mM, 100 mM and 200 mM. The pH of these solutions was adjusted to 4 with HNO_3 as well. Finally, a fixed volume of the stock suspension was added to each one of the electrolyte solutions. The pH of the final suspension was checked before the mobility measurements. The solid concentration of the final suspensions was approximately 0.01 mg/mL.

Electrophoretic mobility measurements. The electrophoretic mobility was measured at room temperature in a Malvern Zetasizer Nano ZS. Each reported data point is the average of 3 or 4 measurements, each one of them carried out on a different 0.8 mL aliquot of the dispersion.

MODEL AND SIMULATION.

Model. In this work, simulations were performed within the primitive model, in which ions are considered charged hard spheres and the solvent is thought of as a continuum of dielectric constant ε_r. Many previous theoretical studies and simulations have proved

Physical Chemistry Chemical Physics Accepted Manuscript

that this representation of reality is able to encompass essential features of real systems and overcome some limitations of the classical electric double layer theory (EDL). In fact, this model has been particularly useful in the study of mesoscopic systems governed by electrostatic interactions as well as the effects of the ionic size.[34–38]

A planar EDL in water (at 298 K) has been simulated here. Such an EDL is generated by a uniformly charged wall (that represents the particle surface) located at z=0. The interaction energy between two ions, i and j, can be split into the electrostatic energy (u_{elec}), the ionic dispersion energy (u_{disp}) and the hard sphere term (u_{hs}), which accounts for the ion size:

$$u(r) = u_{elec}(r) + u_{disp}(r) + u_{hs}(r)$$
$$u_{elec}(r) = \frac{Z_i Z_j e^2}{4\pi\varepsilon_0\varepsilon_r r}$$
$$u_{disp}(r) = -\frac{B_{i/j}}{r^6} \qquad (1)$$
$$u_{hs}(r) = \begin{cases} \infty & r < (d_i + d_j)/2 \\ 0 & r \geq (d_i + d_j)/2 \end{cases}$$

Here d_i and Z_i are the hydrated ion diameter and the valence, respectively, of species i, e is the elementary charge, ε_0 is the permittivity of vacuum, r is the center-to-center distance between ions and $B_{i/j}$ is the parameter characterizing the dispersion interaction between species i and j. More information about this parameter is provided below.

The interaction energy between ions and the colloid surface can also be divided into analogous terms:

$$u_{elec}(z) = -\frac{\sigma_0 Z_i e z}{2\varepsilon_0\varepsilon_r}$$
$$u_{disp}(z) = -\frac{B_{i/m}}{z^3} \qquad (2)$$
$$u_{hs}(z) = \begin{cases} \infty & z < d_i/2 \\ 0 & z \geq d_i/2 \end{cases}$$

Here z is the distance between ion i and the planar surface, σ_0 is the surface charge density, and $B_{i/m}$ is the dispersion parameter corresponding to the interaction between the ionic species i and the magnetite particle. Here, a fixed surface charge density of

Physical Chemistry Chemical Physics Accepted Manuscript

0.075 C/m^2 was employed. This value is approximately that reported by Regazzoni *et al.*[28] for magnetite in aqueous solution, at pH 4 and in the presence of KNO_3 1 mM.

Simulations. The conventional Metropolis algorithm is applied to a canonical ensemble for a collection of N ions confined in a rectangular prism (or cell) of dimensions $W\times W\times L$. More specifically, this simulation cell contains an ionic mixture corresponding to the bulk electrolyte solution together with an excess of counterions neutralizing the surface charge. The impenetrable charged wall is located at z=0 (as mentioned previously) whereas at $z=L$ another impenetrable wall without charge is placed. In addition, periodic boundary conditions were used in the lateral directions (x and y). The system was always thermalized before collecting data for averaging (as usual) and the acceptance ratio was kept between 0.3 and 0.5. The L-values used in our simulations are (at least) one order of magnitude larger than the Debye length. In this way, a considerable portion of the solution bulk is included in the simulation box. The so-called Lekner-Sperb method is applied to account for corrections associated to the long range of the electrostatic interactions in the energy computation. More information about this method and simulations can be found elsewhere. [26,39]

Dispersion constants. As our work focused on the effect of dispersion forces, the values of $B_{anion/anion}$, $B_{anion/cation}$, $B_{cation/cation}$, $B_{anion/m}$ and $B_{cation/m}$ play a key role. According to the Lifshitz theory for van der Waals forces,[23,40] the constant between two ionic species (i and j) can be calculated as:

$$\frac{B_{i/j}}{k_B T} = 3\frac{\alpha_i(0)\alpha_j(0)}{\varepsilon_s^2(0)} + \sum_{n=1}^{\infty}\frac{\alpha_i(\nu_n)\alpha_j(\nu_n)}{\varepsilon_s^2(\nu_n)} \qquad (3)$$

Here k_B is Boltzmann's constant, T is the absolute temperature, $\alpha_i(\nu)$ is the effective polarizability of ion i at water and frequency ν, $\varepsilon_s(\nu)$ is the dielectric constant of the solvent at the same frequency, and $\nu_n = 2\pi k_B T n/h$, where h is Planck's constant and n an integer. Analogously, the dispersion constant characterizing the interaction between a small ion and a colloidal particle (whose surface is assumed to be planar as compared to ions) is given by:

$$\frac{B_{i/m}}{k_B T} = \frac{\alpha_i(0)}{4\varepsilon_s(0)}\left(\frac{\varepsilon_s(0)-\varepsilon_p(0)}{\varepsilon_s(0)+\varepsilon_p(0)}\right) + \sum_{n=1}^{\infty}\frac{\alpha_i(\nu_n)}{2\varepsilon_s(\nu_n)}\left(\frac{\varepsilon_s(\nu_n)-\varepsilon_p(\nu_n)}{\varepsilon_s(\nu_n)+\varepsilon_p(\nu_n)}\right) \qquad (4)$$

Here $\varepsilon_s(\nu)$ is the dielectric constant of the particle (magnetite in our case) at a given frequency ν. As can be seen, this theory requires the knowledge of effective

Physical Chemistry Chemical Physics Accepted Manuscript

polarizabilities and dielectric constants at different frequencies, which can be estimated from the harmonic oscillator model as:

$$\alpha(\nu) = \frac{\alpha(0)}{1+(\nu/\nu_I)^2} \quad (5)$$

$$\varepsilon(\nu) - 1 = \frac{\varepsilon(0)-1}{1+(\nu/\nu_I)^2} \quad (6)$$

Where ν_I is the characteristic frequency of the harmonic oscillator, known in this context as ionization frequency.

Some authors had previously calculated some of the dispersion constants that we needed for our simulations from the Lifshitz theory. Specifically, Tavares *et al.* computed $B_{Na/Na}$ as well as $B_{anion/anion}$ and $B_{anion/Na}$ for ClO_4^- and SO_4^{2-},[23] whereas Boström *et al.* estimated $B_{anion/anion}$ and $B_{anion/Na}$ for SCN^-.[22] In this work, however, we estimated $B_{i/m}$ and $B_{Na/m}$ for magnetite particles and all of the dispersion constants in which citrate ions are involved ($B_{citrate/citrate}$, $B_{citrate/Na}$, $B_{citrate/m}$), since these values have not been found in previous literature.

It should be mentioned that Equation (6) was not applied in the computation of dispersion constants involving magnetite. Instead, an expression published by Faure *et al.*[30] describing the dielectric response of magnetite particles in terms of two characteristic frequencies (ν_{IR} and ν_{UV}) was employed. According to these authors:

$$\varepsilon(\nu) - 1 = \frac{C_{IR}}{1+(\nu/\nu_{IR})^2} + \frac{C_{UV}}{1+(\nu/\nu_{UV})^2} \quad (7)$$

Here C_{IR} and C_{UV} are constants characterizing the corresponding decays. Faure *et al.*[30] also provided the values of these spectral parameters for magnetite as well as other iron oxide phases.

From equations (4), (5), (6) and (7), and the ionization frequencies summarized by Tavares *et al.*,[23] $B_{Na/m}$ and $B_{anion/m}$ for anions ClO_4^- and SO_4^{2-} were calculated. In the case of SCN^- the value of polarizability employed in the computation of $B_{anion/m}$ was previously used by Boström *et al.*[41] Unfortunately, the ionization frequency of this species was not found in in works where the Lifshitz theory was applied to similar

Physical Chemistry Chemical Physics Accepted Manuscript

colloidal systems.[2,22,23,42] In a previous work, Boström *et al.* faced the same problem.[42] After analysing the characteristic frequencies of different ions computed by Mahan *et al.*,[43] these authors concluded that ν_I typically ranges from $1.6 \cdot 10^{15}$ to $8 \cdot 10^{15}$ Hz and estimated the dispersion constants corresponding to these limit values.[42] It can be easily shown from Equation (4) and (5) that $B_{i/m}$ increases with ν_I, which means that the effects of van der Waals forces are stronger for ions with greater characteristic frequencies. For this reason, we preferred to compute $B_{i/m}$ (for the thiocyanate/magnetite pair) corresponding to the upper limit of ν_I.

This ν_I-value was also employed in the computation of the three dispersion constants involving acetate and citrate ions ($B_{acetate/acetate}$, $B_{acetate/Na}$, $B_{acetate/m}$,$B_{citrate/citrate}$, $B_{citrate/Na}$, $B_{citrate/m}$) since the ionization frequency of this species was also unknown for us. The polarizability of acetate ions was extracted from the review by Lo Nostro *et al.*[2] In the case of citrate, an estimate of the static effective polarizability in water was also made as follows. Citrate ions are expected to be the largest anions among those studied in this survey (see next subsection, in which ionic diameters are estimated). In fact, their volume could be twice larger than ClO_4^- and SO_4^{2-}anions, whose static polarizabilities are 5.4 and 6.3 Å^3,[23] respectively. Since the electronic polarizability is proportional to the molecule volume in the harmonic oscillator model, a static polarizability of 10 Å^3 (in round numbers) was assumed for citrate anions. The values of the dispersion constants used in this work are summarized in Table 1.

Ionic diameters. Some previous works clearly suggests that the effects of van der Waals forces are significantly influenced by ion size. We should also bear in mind that ions between the particle surface and the outer Helmholtz plane are expected to be dehydrated. Thus we have considered a simple model for dehydration in our simulations. According to this model, ions trying to cross the outer Helmholtz plane were allowed to reduce their diameters to a bare ion value. Certainly, this is a simple model for dehydration, but it offers the advantage of requiring only one additional parameter (the bare ion size). Table 2 shows the diameters for hydrated and bare ions employed in our simulations. The values corresponding to sodium were straightforwardly extracted from Israelachvili.[40] The bare diameters of ClO_4^-, SCN^-, SO_4^{2-}, $CH_3CH_2OO^-$ and the citrate ion were assumed to be practically identical to the molecular diameters of their acids, which in turn were estimated from the mean molecular volume occupied in the liquid state.[40] The hydrated ion diameters of these

Physical Chemistry Chemical Physics Accepted Manuscript

anions were estimated adding up the thickness of a hydration layer similar to that of NO_3^-, 0.08 nm.[40]

Charge of citrate ions. Although experiments were carried out at pH=4, we should keep in mind that the local pH near the surface of a positively charged colloidal particle is expected to be larger (since the concentration of $H_3O^+$is smaller than in the bulk of the solution). As the pK_a of the second and the third proton of the citric acid are 4.77 and 6.70, respectively, we have assumed that the doubly charged citrate anions are the predominant species.

Computation of the diffuse potential. The diffuse potential (ψ_d) is defined as the electric potential at the plane of closest approach of the hydrated ions to the charged surface (the outer Helmholtz plane). This EDL property is extremely useful in comparing with experiments, since it is intimately related to the ζ-potential, which is a crucial quantity to analyse electrokinetic phenomena. From the ionic profiles provided by simulations, the diffuse potential of a planar EDL can be computed as follows:

$$\psi_d \equiv \psi(d_1/2) = \frac{e}{\varepsilon_r \varepsilon_0} \int_{d_1/2}^{\infty} (d_1/2 - z) \sum_i Z_i \rho_i(z) dz \qquad (8)$$

where d_1 is the hydrated ion diameter of counterions and $\rho_i(z)$ is the local density of i-ions at a distance z from the charged surface. Some practical guidelines for the application of this equation to simulation data were provided in previous papers.[26,39]

RESULTS

Magnetite Nanoparticles. The magnetite nanoparticles were predominantly octahedral, with a typical size of 50 nm (see figure 1), which is in agreement with previous synthesis processes[33] carried out also in an excess of OH^- of 0.075 M. It was determined in that study that these octahedral particles were single crystals, that their stoichiometry corresponded to a slightly oxidized form of magnetite, and that their saturation magnetization was ca. 82 emu/g at room temperature.

Physical Chemistry Chemical Physics Accepted Manuscript

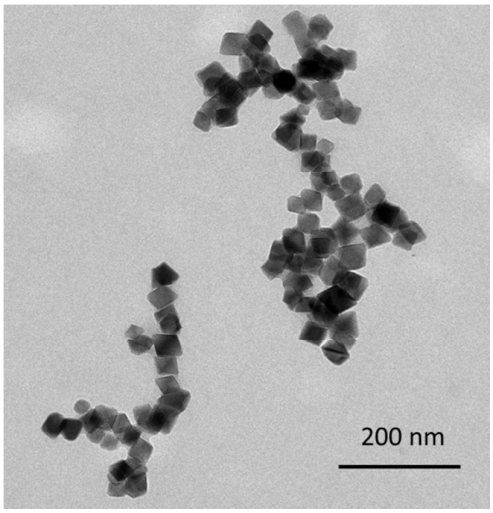

Figure 1. *TEM micrograph of the iron oxide nanoparticles prepared by oxidation of ferrous hydroxide with KNO_3 in an excess of OH^-.*

Electrophoretic mobility. Measurements of the electrophoretic mobility (μ) as a function of pH were carried out to ensure that our nanoparticles' electrokinetic behaviour was similar to that reported for magnetite in the literature. From the resulting curve, shown in Figure 2, we concluded that the isoelectric point of our particles was in the vicinity of 6.7. This is in good agreement with previous observations by our group[44] and with the values reported for the isoelectric point of magnetite (Fe_3O_4) by Regazzoni *et al*.[28] and by Vidojkovic *et al*.[29] Note that these two articles included a collection of *point of zero charge* (PZC) and *isoelectric point* (IEP) data for magnetite taken from the literature, and that most of those data are between pH = 6.5 and pH = 7.0.

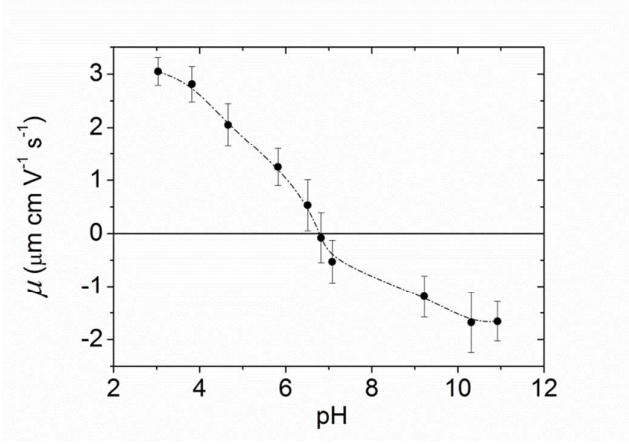

Figure 2. *Electrophoretic mobility of the magnetite nanoparticles as a function of pH. Nanoparticles were dispersed in a 2 mM KNO_3 solution. The pH was adjusted with NaOH or HNO_3. Line is provided as guide to the eye.*

Physical Chemistry Chemical Physics Accepted Manuscript

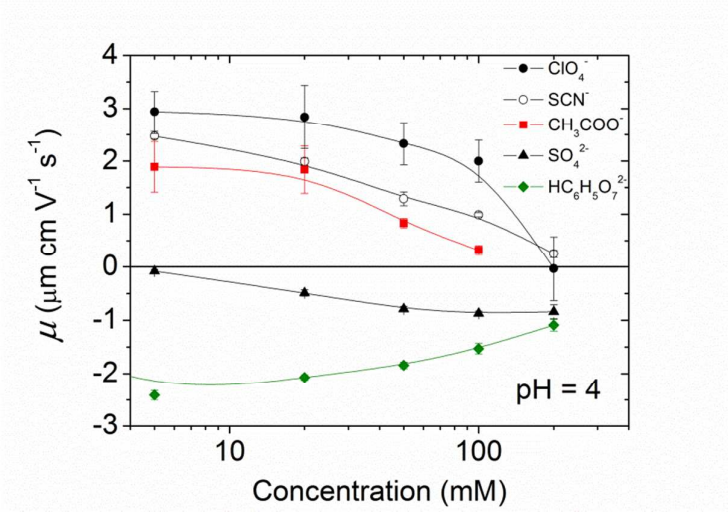

Figure 3. *Electrophoretic mobility of the magnetite nanoparticles in the presence of different anions. The cation was always* Na^+ *and the pH was fixed with* HNO_3.

The evolution of the electrophoretic mobility (μ) of the magnetite nanoparticles, at pH = 4, and as a function of the concentration of different anions, is shown in Figure 3. At pH 4 and in the absence of any electrolyte other than the nitrate ions and the protons from the nitric acid used to fix the pH, μ was approximately 3.0 μm cm V^{-1} s^{-1}. In all cases the addition of an electrolyte lowered that mobility due to a decrease of the effective positive surface charge of the particles as the counterions (anions) approach the surface. However, we observed a very different behaviour between the chaotropic (SCN^-, ClO_4^-, see the representative Hofmeister series given in the introduction) and the kosmotropic (SO_4^{2-}, $HC_6H_5O_7^{2-}$) anions. The effect of the chaotropic anions was limited to the screening of the particles' surface charge, bringing μ practically to zero, whereas the kosmotropic anions induced a mobility reversal that was especially fast (i.e it was noticeable at remarkably low anion concentrations) in the case of the citrate ion.

In general, the effectiveness of the anions at decreasing the mobility of the particles follows the Hofmeister series given in the introduction. Only the position of the anions ClO_4^- and SCN^- seems to be exchanged regarding the original Hofmeister series. However, this anomalous behaviour has already observed for other hydrophilic colloids by López-León *et al.*[45] Therein, Hofmeister effects on the electrokinetics and stability of a cationic latex covered with a protein (IgG) were extensively analysed, being the

Physical Chemistry Chemical Physics Accepted Manuscript

anomalous behaviour of SCN^- explained in terms of entropic mechanisms associated with rearrangements in the water structure. Building on this, the authors claimed that the chaotropic/kosmotropic concept can be readily extended from ions to any type of surface. This means that the behavior of hydrophilic surfaces is similar to that of kosmotropic ions, in the sense that they interact strongly with neighboring solvent molecules and promote their ordering, whereas hydrophobic surfaces behave like a chaotropic (structure-breaking) system. This entropically controlled process would explain why the adsorption of chaotropic ions is favoured in hydrophobic surfaces and precluded in hydrophilic ones.[45]

The mobility reversals observed in Figure 3 deserve further discussion. Mobility reversals of colloids induced by counterions have been extensively reported in the literature.[46–52] In general, they were induced by multivalent counterions, high surface charge densities and high salt concentrations. Under such conditions, the phenomenon of mobility reversal can be justified in terms of ion-ion correlations.[53–55] However, the reversal of charged colloids induced by monovalent ions or very low multivalent salt concentrations is much scarcer and cannot be explained in terms of ionic correlations, thus other mechanisms are suggested.[17,25,56–58] For instance, in the case of soft particles made of polyelectrolyte-grafted colloids, the mobility reversal observed in the presence of monovalent salt is governed by the properties of the grafted layer,[58] whereas the reversals of anionic liposomes at low concentrations of trivalent cations were explained in terms of solvent mediated effects.[59] In the case of hard particles, mobility reversal induced by monovalent ions can be dominated by the chaotropic/kosmotropic character of ions and the hydrophobic/hydrophilic character of surfaces.[25,57] In our case, only sulphate and the citrate anions induce negative mobilities of iron oxide particles. The rest of monovalent salts do not induce this phenomenon.

The singular behavior of the mobility measured in the presence of citrate can be explain in terms of i) a strong chemical affinity between the citrate ion and the surface of magnetite, which leads to a large charge reversal at relatively low concentrations of the ion; and by ii) screening of the particle's charge as the ion concentration increases, which results in a decrease of the magnitude of the mobility. The affinity of the carboxyl groups for the surface of iron oxides is well known.[60,61] This affinity depends on the structure of the particular organic acid, but in the case of citrate seems to lead to the formation of metal–carboxylate surface complexes.[62] In fact, citric acid has been routinely (and even commercially) used for the stabilization of iron oxide magnetic

Physical Chemistry Chemical Physics Accepted Manuscript

nanoparticles[10]. Citrate adsorbs on the iron oxide surface, leaving at neutral pH at least one carboxylic group exposed to the solution, which charges negatively the surface and provides stabilization. The behaviour of the mobility in the presence of sulphate follows a trend clearly different from that of the citrate curve, but in agreement with that observed on multivalent ions on other colloidal systems[50,52]: there is a reversal of sign in the mobility and the reversed mobility increases in magnitude with ion concentration, until eventually reaches a plateau. Interestingly, the affinity of the sulphate ion for the surface of the iron oxides is not so well known, but specific adsorption of sulphate was reported by Breeuwsma and Lyklema[13] for hematite particles and by Andres-Verges *et al*.[63] for magnetite particles that were synthesized following a method very similar to ours. These latter authors confirmed the presence of sulphate ions by means of infrared spectroscopy, and concluded that the ions were strongly attached since they were not eliminated by washing in water under sonication, or even after a treatment with hydrochloric acid.

Simulation results. It is quite instructive to find out to what extent the electrokinetic behaviour described above can be justified (and even predicted) from the polarizabilities and the size of the different ions involved. To tackle this issue, the diffuse potentials of a planar magnetite surface in the presence of different concentrations of the same ions used in electrophoresis experiments were calculated by means of MC simulations (figure 4).

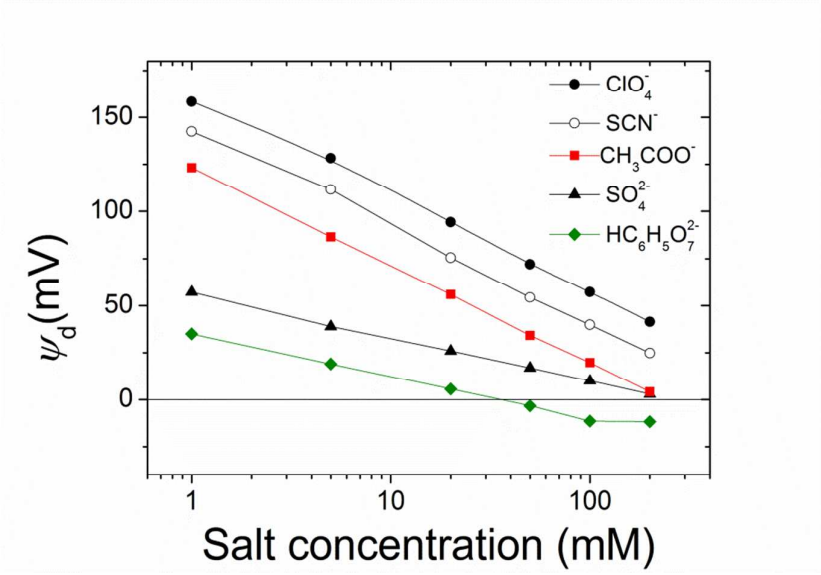

Figure 4. *Diffuse potential calculated by MC simulations, as a function of concentration of salt for the same anions used in Figure 3. Input data for simulations are shown in tables 1 and 2.*

Physical Chemistry Chemical Physics Accepted Manuscript

Assuming that tendencies for ψ_d should be similar to those found experimentally for μ, a qualitative comparison between both magnitudes can be done. As can be seen, there are different curves for ions with the same valence, which evidences the specificity in the interaction of these ions with the magnetite. What is more, the general trends shown in Figure 3 are captured by simulations. More specifically, the Hofmeister series for hydrophilic systems exhibited by our particles in experiments is also observed in simulation results: $\psi_d(ClO_4^-) > \psi_d(SCN^-) > \psi_d(CH_3COO^-) > \psi_d(SO_4^{2-}) > \psi_d(HC_6H_5O_7^{2-})$. This means that chaotropic ions screened the charge of the particles more feebly than the kosmotropic ones. We could also mention that a diffuse potential reversal was reached in simulations. However, this reversal was only found for $HC_6H_5O_7^{2-}$ at moderate and high salt concentrations, whereas mobility reversals were clearly observed for citrate and sulphate anions over a wider range of electrolyte concentrations. This qualitative difference between experiments and simulations will be discussed later in more detail.

Now let us elaborate on the simulation results shown in Figure 4. Although the agreement between simulation predictions and experimental data is only qualitative, it is important to emphasize that the specific ion effects that characterize the electrokinetic behaviour of iron oxide particles were reproduced by simulations without requiring any fitting parameters. We should also keep in mind that input data used in simulations shown in tables 1 and 2 were estimated from Lifshitz theory for van der Waals forces and from the literature, respectively (see Model and Simulations section). Undoubtedly, the qualitative resemblance between Figures 3 and 4 supports the capability of prediction of this theoretical approach.

Additionally, it suggests that ionic polarizabilities and sizes play a key role in justifying the ionic specificity observed. In other words, these two magnitudes are responsible to a great extent for the specific effects of Hofmeister series on the electrokinetic potential of oxide iron particles. This finding agrees with the general assumptions of the most recent theories on surface hydration, which combined with hydrated nonelectrostatic potentials, have been developed to predict experimental zeta potentials and hydration forces.[5]

Now, let us turn to the discrepancies in the charge reversal phenomena found in the experiments and in the simulations. It is evident that mobility reversal induced by kosmotropic anions is not properly predicted by simulations. SO_4^{2-} and $HC_6H_5O_7^{2-}$

Physical Chemistry Chemical Physics Accepted Manuscript

anions induce a clear reversal in the sign of μ whereas the diffuse potential reversal is only achieved in the presence of $HC_6H_5O_7^{2-}$ anions at moderate and high electrolyte concentrations, as mentioned before. At this point it is appropriate to recall that mobility reversal and potential reversal may not be necessarily equivalent. The reader should bear in mind that the diffuse potential was evaluated at the plane of closest approach of the hydrated ions to the charged surface, also called Outer Helmholtz plane (OHP). On the other hand, electrophoresis mobility is associated to ζ-potential defined in the shear plane. Although the approximation $\psi_d \approx \zeta$ is acceptable for ideal surfaces, the OHP and shear planes are not the strictly the same. For real colloids, shear plane is expected to be further from the surface than the OHP.[64] Accordingly, the salt concentration at which mobility reversal was experimentally reached would not correspond to that required to induce a reversal in the diffuse potential. In order to illustrate this feature, the electrostatic potential was calculated as a function of the distance from the magnetite surface (normalized by the ionic diameter) in the presence of SO_4^{2-} anions at 100 and 200 mM concentrations (Figure 5).

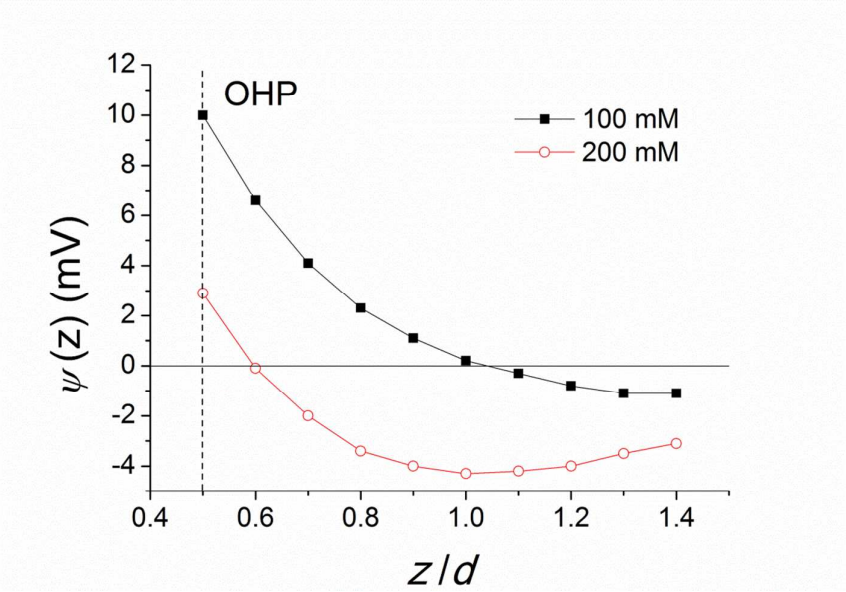

Figure 5*. Electrostatic potential calculated by MC simulations as a function of the distance from the surface for two concentrations of SO_4^{2-}. Input data for simulations are shown in tables 1 and 2.*

As can be seen in Figure 5, the electrostatic potential at the OHP is always positive. However, for larger distances from the surface, a potential reversal can be reached, especially for the highest salt concentrations. Accordingly, better agreement with

Physical Chemistry Chemical Physics Accepted Manuscript

experiments would have been observed if an electrostatic potential further from the surface had been used to characterize electrokinetic phenomena. Indeed, this approach was employed in a previous work in which diffuse potentials, theoretically calculated from an integral equation theory, fit mobility reversal data of latex particles.[65] Nevertheless, since the distance between the OHP and the shear plane is not clearly identified, this magnitude would become a fitting parameter in the calculations, and this procedure would reduce the predictive effectiveness of simulations and we preferred to avoid it.

In a previous paragraph, the diverse origins of the mobility reversals previously described in literature were briefly commented. In this sense, it would be interesting to look into the origin of the reversal of the diffuse potential of magnetite nanoparticles observed in simulations in the presence of citrate anions. Given that this species was assumed to be divalent, the role of ion-ion correlations might be important. Computer simulations are extremely useful to shed light on this kind of issues since some interactions can be deliberately *switched off*. For instance, Figure 6 shows the diffuse potential obtained in the presence of citrate anions if all the dispersion constants vanish and dispersion interactions are left out. The figure also included the results previously obtained for citrate anions and perchlorate anions, as a reference of monovalent species in which the reduction of diffuse potential caused by dispersion forces is not intense. Let us focus on the results obtained in the absence of dispersion forces. As can be seen, when the valence of the anion is doubled (changing perchlorate into citrate ions), the diffuse potential considerably decreases but this curve does not exhibit change of sign. The reversal only appears when dispersion forces are additionally *switched on*. This suggests that ion-ion correlations cannot justify the change of sign on its own.

Physical Chemistry Chemical Physics Accepted Manuscript

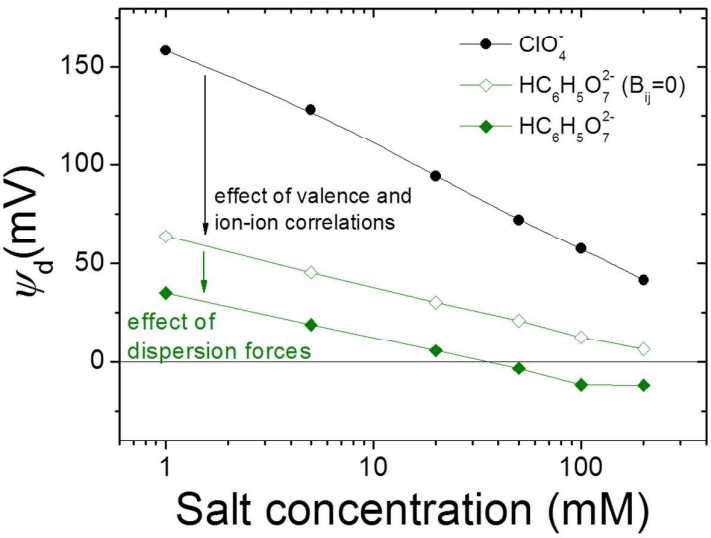

***Figure 6**. Diffuse potential calculated by MC simulations with and without dispersion forces in the presence of citrate anions as a function of the electrolyte concentration. Results for perchlorate ions are also plotted for comparison.*

Finally, we are aware that the primitive model is a quite simple to accurately explain ion specific effects in colloidal systems. It leaves out many effects that could sometimes not be negligible and more sophisticated models that include quantum dispersion forces are required. We could have also considered the affinity of the carboxyl groups and the sulphate ions for the surface of iron oxides, previously mentioned, in our simulations. The inclusion of this interaction would probably improve the agreement between experiment and simulations, but it would require the use of interaction parameters not known *a priori*. Actually, the fact that simulations did not take into account that chemical affinity could explain the discrepancy between the trends of the experimental and the simulations citrate curves. It should be noted that the main difference between the curves is the larger mobility inversion measured at low ion concentrations, which, as mentioned above, is related to the chemisorption of the citrate ion on the iron oxide surface.

Physical Chemistry Chemical Physics Accepted Manuscript

CONCLUSIONS.

We observed ion specificity phenomena in colloidal suspensions of magnetite nanoparticles. Concretely, the electrophoretic mobility of the magnetite particles evolved very differently when exposed to increasing concentrations of different anions. The effect of an increasing concentration of chaotropic anions was milder and was limited to a screening of the charge until the mobility was negligible. On the contrary, kosmotropic anions reduced the positive charge more effectively and caused a mobility inversion even at low concentrations. If the anions were ordered according to their effectiveness at decreasing the positive charge of the particles, they followed a Hofmeister series, with the exception of SCN^- and ClO_4^- ions, which had their positions exchanged. This exception had been observed also by López-León and coworkers[45] in some cationic hydrophilic colloids. It should be reminded that the bare surface of magnetite is known to be hydrophilic and positively charged at pH 4.

Monte Carlo simulations were used to gain more insight into the origin of the behavior of different anions. Qualitatively speaking, the diffuse potential predicted for them from the Lifshitz theory for van der Waals forces exhibited features very similar to those found in the electrophoretic mobility experiments. In particular, the same Hofmeister series was observed for the diffuse potential, which supports that simulations provide a useful tool to qualitatively predict the ionic specificity on the electrokinetic behavior of iron oxide particles and other colloidal particles. Simulations also suggested that the polarizability of citrate ions and the associated dispersion forces play and important role in justifying the reversal observed in the presence of these anions, at least at high salt concentrations.

ACKNOWLEDGEMENTS.

The authors thank the financial support from the following institutions: i) 'Ministerio de Economía y Competitividad, Plan Nacional de Investigación, Desarrollo e InnovaciónTecnológica (I+D+i)', Projects MAT2013-44429-R, MAT2012-36270-C04-04 and -02. ii) 'Consejería de Innovación, Ciencia y Empresa de la Junta de Andalucía', Projects P09-FQM-4698, P10-FQM-5977, and P11-FQM-7074. iii) European Regional

Physical Chemistry Chemical Physics Accepted Manuscript

Development Fund (ERDF). Fernando Vereda is especially grateful to the "Programa de Reincorporación de Doctores" of the Universidad de Granada. The helpful discussions of Dr. Ortega-Vinuesa are also sincerely acknowledged.

Physical Chemistry Chemical Physics Accepted Manuscript

REFERENCES

1 A. Salis and B. W. Ninham, *Chem. Soc. Rev.*, 2014, **43**, 7358–77.

2 P. Lo Nostro and B. W. Ninham, *Chem. Rev.*, 2012, **112**, 2286–322.

3 J. Lyklema, *Chem. Phys. Lett.*, 2009, **467**, 217–222.

4 W. Kunz, P. Lo Nostro and B. W. Ninham, *Curr. Opin. Colloid Interface Sci.*, 2004, **9**, 1–18.

5 D. F. Parsons, M. Boström, P. Lo Nostro and B. W. Ninham, *Phys. Chem. Chem. Phys.*, 2011, **13**, 12352–67.

6 A. Salis, F. Cugia, D. F. Parsons, B. W. Ninham and M. Monduzzi, *Phys. Chem. Chem. Phys.*, 2012, **14**, 4343–4346.

7 P. Jungwirth and D. J. Tobias, *Chem. Rev.*, 2006, **106**, 1259–81.

8 S. Bae, H. Son, Y.-G. Kim and S. Hohng, *Phys. Chem. Chem. Phys.*, 2013, **15**, 15829–15832.

9 P. Tartaj, M. P. Morales, T. Gonzalez-Carreño, S. Veintemillas-Verdaguer and C. J. Serna, *Adv. Mater.*, 2011, **23**, 5243–5249.

10 K. Turcheniuk, A. V Tarasevych, V. P. Kukhar, R. Boukherroub and S. Szunerits, *Nanoscale*, 2013, **5**, 10729–52.

11 M. Colombo, S. Carregal-Romero, M. F. Casula, L. Gutiérrez, M. P. Morales, I. B. Böhm, J. T. Heverhagen, D. Prosperi and W. J. Parak, *Chem. Soc. Rev.*, 2012, **41**, 4306.

12 F. Dumont and A. Watillon, *Discuss. Faraday Soc.*, 1971, **52**, 352–360.

13 A. Breeuwsma and J. Lyklema, *J. Colloid Interface Sci.*, 1973, **43**, 437–448.

14 M. Čolić, D. W. Fuerstenau, N. Kallay and E. Matijević, *Colloids and Surfaces*, 1991, **59**, 169–185.

15 D. R. Dixon, *Colloids and Surfaces*, 1985, **13**, 273–286.

16 M. Boström, D. Williams and B. Ninham, *Phys. Rev. Lett.*, 2001, **87**, 168103.

17 T. López-León, A. B. Jódar-Reyes, D. Bastos-González and J. L. Ortega-Vinuesa, *J. Phys. Chem. B*, 2003, **107**, 5696–5708.

18 P. H. R. Alijó, F. W. Tavares and E. C. B. Jr., *Colloids Surfaces A Physicochem. Eng. Asp.*, 2012, **412**, 29–35.

Physical Chemistry Chemical Physics Accepted Manuscript

19 F. W. Tavares, M. Boström, E. R. A. Lima and E. C. Biscaia, *Fluid Phase Equilib.*, 2010, **296**, 99–105.

20 E. R. a Lima, F. W. Tavares and E. C. Biscaia, *Phys. Chem. Chem. Phys.*, 2007, **9**, 3174–3180.

21 V. Deniz, M. Boström, D. Bratko, F. W. Tavares and B. W. Ninham, *Colloids Surfaces A Physicochem. Eng. Asp.*, 2008, **319**, 98–102.

22 M. Boström, F. W. Tavares, B. W. Ninham and J. M. Prausnitz, *J. Phys. Chem. B*, 2006, **110**, 24757–60.

23 F. Tavares and D. Bratko, *J. Phys. Chem. B*, 2004, **108**, 9228–9235.

24 E. R. A. Lima, D. Horinek, R. R. Netz, E. C. Biscaia, F. W. Tavares, W. Kunz and M. Boström, *J. Phys. Chem. B*, 2008, **112**, 1580–5.

25 C. Calero, J. Faraudo and D. Bastos-González, *J. Am. Chem. Soc.*, 2011, **133**, 15025–15035.

26 A. Martín-Molina, J. G. Ibarra-Armenta and M. Quesada-Pérez, *J. Phys. Chem. B*, 2009, **113**, 2414–21.

27 M. Quesada-Pérez, R. Hidalgo-Álvarez and A. Martín-Molina, *Colloid Polym. Sci.*, 2010, **288**, 151–158.

28 A. E. Regazzoni, M. A. Blesa and A. J. G. Maroto, *J. Colloid Interface Sci.*, 1983, **91**, 560–570.

29 S. Vidojkovic, V. Rodriguez-Santiago, M. V. Fedkin, D. J. Wesolowski and S. N. Lvov, *Chem. Eng. Sci.*, 2011, **66**, 4029–4035.

30 B. Faure, G. Salazar-alvarez and L. Bergström, *Langmuir*, 2011, **27**, 8659–8664.

31 T. Sugimoto and E. Matijevic, *J. Colloid Interface Sci.*, 1980, **74**, 227–243.

32 F. Vereda, J. de Vicente and R. Hidalgo-Alvarez, *J. Colloid Interface Sci.*, 2013, **392**, 50–6.

33 F. Vereda, J. De Vicente, M. Del Puerto Morales, F. Rull and R. Hidalgo-Álvarez, *J. Phys. Chem. C*, 2008, **112**, 5843–5849.

34 M. Dijkstra, *Curr. Opin. Colloid Interface Sci.*, 2001, **6**, 372–382.

35 P. Linse, *Adv. Polym. Sci.*, 2005, **185**, 111–162.

36 A. V Dobrynin, *Curr. Opin. Colloid Interface Sci.*, 2008, **13**, 376–388.

37 R. Kovács, M. Valiskó and D. Boda, *Condens. Matter Phys.*, 2012, **15**, 23803.

Physical Chemistry Chemical Physics Accepted Manuscript

38 M. Valiskó, D. Henderson and D. Boda, *Condens. Matter Phys.*, 2013, **16**, 43601.

39 M. Quesada-Pérez, A. Martín-Molina and R. Hidalgo-Alvarez, *J. Chem. Phys.*, 2004, **121**, 8618–26.

40 J. N. Israelachvili, *Intermolecular and surface forces / Jacob N. Israelachvili*, Academic Press, London ; San Diego :, 1991.

41 M. Boström, D. Parsons and A. Salis, *Langmuir*, 2011, **27**, 9504–9511.

42 M. Boström, D. Williams and B. Ninham, *Biophys. J.*, 2003, **85**, 686–694.

43 G. D. Mahan, *J. Chem. Phys.*, 1982, **76**, 493.

44 F. Vereda, J. de Vicente and R. Hidalgo-Álvarez, *Colloids Surfaces A Physicochem. Eng. Asp.*, 2008, **319**, 122–129.

45 T. López-León, M. J. Santander-Ortega, J. L. Ortega-Vinuesa and D. Bastos-González, *J. Phys. Chem. C*, 2008, **112**, 16060–16069.

46 R. . Ottewill and J. . Shaw, *J. Colloid Interface Sci.*, 1968, **26**, 110–119.

47 M. Elimelech and C. R. O'Melia, *Colloids and Surfaces*, 1990, **44**, 165–178.

48 M. Tanaka and A. Y. Grosberg, *J. Chem. Phys.*, 2001, **115**, 567.

49 M. Quesada-Pérez, A. Martín-Molina, F. Galisteo-González and R. Hidalgo-Álvarez, *Mol. Phys.*, 2002, **100**, 3029–3039.

50 A. Martín-Molina, M. Quesada-Pérez, F. Galisteo-González and R. Hidalgo-Álvarez, *Colloids Surfaces A Physicochem. Eng. Asp.*, 2003, **222**, 155–164.

51 K. Besteman, M. A. G. Zevenbergen, H. A. Heering and S. G. Lemay, *Phys. Rev. Lett.*, 2004, **93**.

52 A. Martín-Molina, J. A. Maroto-Centeno, R. Hidalgo-Álvarez and M. Quesada-Pérez, *Colloids Surfaces A Physicochem. Eng. Asp.*, 2008, **319**, 103–108.

53 A. Y. Grosberg, T. T. Nguyen and B. I. Shklovskii, *Rev. Mod. Phys.*, 2002, **74**, 329–345.

54 Y. Levin, *Reports Prog. Phys.*, 2002, **65**, 1577–1632.

55 M. Quesada-Pérez, E. González-Tovar, A. Martín-Molina, M. Lozada-Cassou and R. Hidalgo-Alvarez, *Chemphyschem*, 2003, **4**, 234–48.

56 T. López-León, a. B. Jódar-Reyes, J. L. Ortega-Vinuesa and D. Bastos-González, *J. Colloid Interface Sci.*, 2005, **284**, 139–148.

Physical Chemistry Chemical Physics Accepted Manuscript

57 A. Martín-Molina, C. Calero, J. Faraudo, M. Quesada-Pérez, A. Travesset and R. Hidalgo-Álvarez, *Soft Matter*, 2009, 5, 1350.

58 S. Raafatnia, O. A. Hickey and C. Holm, *Phys. Rev. Lett.*, 2014, **113**, 238301.

59 A. Martín-Molina, C. Rodríguez-Beas and J. Faraudo, *Phys. Rev. Lett.*, 2010, **104**, 168103.

60 L. Shen, P. E. Laibinis and T. A. Hatton, *ACS Macro Lett.*, 1999, **15**, 447–453.

61 A. Wooding, M. Kilner and D. B. Lambrick, *J. Colloid Interface Sci.*, 1991, **144**, 236–242.

62 E. Tombácz, I. Y. Tóth, D. Nesztor, E. Illés, A. Hajdú and M. Szekeres, *Colloids Surfaces A Physicochem. Eng. Asp.*, 2013, **435**, 91–96.

63 M. Andrés Vergés, R. Costo, a G. Roca, J. F. Marco, G. F. Goya, C. J. Serna and M. P. Morales, *J. Phys. D. Appl. Phys.*, 2008, **41**, 134003.

64 R. J. Zasoski, in *Encyclopedia of Soil Science SE - 644*, ed. W. Chesworth, Springer Netherlands, 2008, pp. 841–845.

65 A. Martín-Molina, M. Quesada-Perez, F. Galisteo-Gonzalez and R. Hidalgo-Alvarez, *Trends Colloid Interface Sci. Xvi*, 2004, **123**, 114–118.

Physical Chemistry Chemical Physics Accepted Manuscript

Table 1. Dispersion constants used in our simulations for different electrolytes.

Electrolyte	$\frac{B_{anion/anion}}{k_BT}$ (nm^6)	$\frac{B_{anion/cation}}{k_BT}$ (nm^6)	$\frac{B_{cation/cation}}{k_BT}$ (nm^6)	$\frac{B_{anion/m}}{k_BT}$ (nm^3)	$\frac{B_{cation/m}}{k_BT}$ (nm^3)
Na_2SO_4	$4.69 \cdot 10^{-3}$	$2.01 \cdot 10^{-4}$	$1.31 \cdot 10^{-5}$	$1.27 \cdot 10^{-2}$	$1.83 \cdot 10^{-3}$
$NaClO_4$	$1.59 \cdot 10^{-3}$	$8.97 \cdot 10^{-5}$	$1.31 \cdot 10^{-5}$	$4.07 \cdot 10^{-3}$	$1.83 \cdot 10^{-3}$
NaSCN	$4.69 \cdot 10^{-3}$	$2.00 \cdot 10^{-4}$	$1.31 \cdot 10^{-5}$	$6.34 \cdot 10^{-2}$	$1.83 \cdot 10^{-3}$
NaAcetate	$3.86 \cdot 10^{-4}$	$11.0 \cdot 10^{-6}$	$1.31 \cdot 10^{-5}$	$6.43 \cdot 10^{-2}$	$1.83 \cdot 10^{-3}$
NaCitrate	$1.28 \cdot 10^{-3}$	$2.00 \cdot 10^{-5}$	$1.31 \cdot 10^{-5}$	$11.7 \cdot 10^{-2}$	$1.83 \cdot 10^{-3}$

Table 2. Ionic diameters used in our simulations.

Ión	Bare ion diameter (nm)	Hydrated ion diameter (nm)
Na^+	0.19	0.72
ClO_4^-	0.52	0.68
SO_4^{2-}	0.50	0.66
SCN^-	0.40	0.56
CH_3COO^-	0.51	0.67
Citrato	0.65	0.81

Physical Chemistry Chemical Physics Accepted Manuscript